Langmuir circulations beneath growing or decaying surface waves

By W. R. C. PHILLIPS

Department of Theoretical and Applied Mechanics
University of Illinois at Urbana-Champaign, Urbana, IL 61801-2935, USA.

(Received 3 January 2001; wrphilli@uiuc.edu)

The instability to longitudinal vortices of an evolving two dimensional weakly sheared density stratified wavy flow is considered. The problem is posited in the context of Langmuir circulations, LC's, beneath irrotational wind driven surface waves and the instability mechanism is Craik-Leibovich type 2, or CL2. Of interest is the influence of temporal waves to the instability according to linear theory. Waves aligned both with the wind and counter to it are considered as is the role of stratification. The basis for the study is a generalization of an initial value problem posed by Leibovich & Paolucci (1981) in which the liquid substrate is of semi-infinite extent and the current is permitted to grow. Here the current has two components: a wind driven portion owing to the wind stress applied at the free surface and a second due to the diffusion of momentum owing to the wave amplitude squared free surface stress condition. In general, it is found that growing waves are stabilizing while decaying waves are destabiizing to the formation of LC's, although the latter applies only for sufficiently large spanwise spacings and is subject to a globally stable lower bound. Decaying waves in the absence of wind can also be destabilizing to LC's. When the wind is counter to the waves, however, only decaying waves are unstable to LC's. Furthermore, while growing waves are stable to the formation of LC's in the presence of stable stratification, decaying waves are unstable in both aligned and opposed windwave conditions. Unstable stratification of the other hand, is destabilizing to LC's for all temporal waves in both aligned and opposed wind-wave conditions.

1. Introduction

Langmuir circulations, or LC's, are organized convective motions that form in the surface layer of oceans, lakes and ponds when winds of moderate strength blow over them. In each instance they manifest as a parallel series of counterrotating vortices that more or less align with the wind (Langmuir 1938). Moreover, they act at the surface to concentrate flotsam, seaweed and air bubbles into clearly visible streaks or bands, with spacings ranging from a few millimeters (Kenney 1993) to several hundred meters (Plueddemann *et al* 1996). Many attempts have been made to explain LC's (see reviews by Leibovich 1983 and Gargett 1989), in part because their apparently ordered structure suggests they may be deterministic, but also because they are thought to be largely responsible for the formation of thermoclines and the maintenance of mixed layers in lakes and oceans. Indeed, in view of the importance of the mixed layer and the heat, mass and momentum transport processes therein (see *e.g.* Li *et al* 1995), the notion of modelling LC's with a view to their inclusion in Global change models is compelling.

Of the suggested range of models to explain LC's, the most plausible have as their basis a nonlinear interaction between surface gravity waves and a weak current; and of interest here is the prevailing theory in this category, that of Craik & Leibovich (1976). These authors provide a rational derivation of a set of equations - the CL-equations - thought to govern LC's, given an $O(\epsilon^2)$ rotational mean current and an irrotational wave field of wave slope $O(\epsilon)$. The CL-equations also follow from

Andrews & McIntyre's (1978) exact theory of nonlinear waves on a Lagrangian-mean flow (Leibovich 1980), in which the nonlinear interaction of the waves with themselves is represented as a rectified effect through the $O(\epsilon^2)$ Stokes drift.

Interestingly, the CL-equations predict that activity akin to Langmuir circulations may result from either of two instability mechanisms, CL1 or CL2. CL1 requires a surface wave field with a high degree of spatial structure, whereas CL2 acts without special spatial structure (Craik 1977, Leibovich 1977a). As discussed in §2.1, of particular relevance in the open ocean is CL2, and this instability has formed the basis of numerous studies concerned with LC's, and the effect to them of stratification, nonlinearity and streamwise growth (*e.g.* Leibovich & Paolucci 1980, 1981; Leibovich *et al* 1989; Cox *et al* 1992; Cox & Leibovich 1993, 1997; Li & Garrett 1993, 1997; Skyllingstad & Denbo 1995; McWilliams *et al* 1997, Phillips 2001b).

Meanwhile test cases for such theories have resulted from an extensive observational program of ocean LC's. (Thorpe & Hall, 1982; Weller *et al* 1985; Smith *et al* 1987; Weller & Price, 1988; Zendel & Farmer, 1991, Smith 1992, 1998; Plueddemann *et al* 1996 and others). But although some observations can be explained by CL2-theory (see *e.g.* Phillips 2001b), studies employing it have, to this point, assumed neutral waves, whereas the waves in field studies on occassion grow or decay. For example, Plueddemann *et al* report an instance where LC's are sustained by slowly decaying waves for tens of hours after an abrupt reduction in the local wind stress. Thus the focus of the present work is to explore the role growing or decaying waves play in the formation of LC's.

In such instances the Stokes drift is a function of time and, in the context of CL2, which is described kinematically in §7, has two components: one aligned with the direction of wave propagation and the second normal to the free surface. Of course the CL-equations still describe the problem, but rather than recasting them (to ensure the correct ordering of terms containing the extra component of Stokes drift), we instead refer to the general set of evolution equations pertinent to the CL2 instability by Phillips (1998), his (4.1). This set were derived from the GLM-equations and are valid for growing rotational or irrotional waves in any level of shear (see §2.1).

Of course unsteadiness of the primary wave field or base flow implies that the linear instability problem is non-separable. Nevertheless, Foster (1965) and Homsy (1973) have deduced techniques that yield precise stability limits in such cases; and Craik (1977) and thence Leibovich & Paulucci (1981), henceforth LP, have exploited such techniques in the context of LC's.

LP consider the formation of LC's via CL2 in an initially quiescent liquid which is subject to acceleration at its free surface by a wind stress. In essence, they take the view that the instability works its way down from the surface, following the imposition there of a wave field and a wind stress; the layer may be then thought of as infinitely deep and the shear within it to resemble a Rayleigh stress layer. They then question the instability of the shear layer at a specified instant in its evolution, in the presence of, since they ignore time evolution of the surface wave field, a stationary Stokes drift field.

Craik (1982a), however, notes that the shear layer is in fact made up of two mean components: one arising from the diffusion of momentum owing to the applied wind stress and a second owing to the viscous diffusion of momentum due to the wave amplitude squared surface stress condition (see §3.1). This means, since the second component is always present, that the flow may be unstable to LC's via CL2 even in the absence of wind, a result consonant with Plueddemann *et al* 's aforementioned observation. It further means that we can credibly allow for both growing and decaying waves; the former propagating in the direction of the wind, the latter propagating counter to it, or in no wind.

Thus, in the present paper, we question the instability *via* CL2, of an evolving shear layer in the presence of a temporal Stokes drift field. The paper is organized as follows: the initial value problem is posed in §2 with details of the primary fields, *i.e.* the mean Eulerian shear layer and mean Lagrangian (Stokes drift) fields given in §3. We then investigate the instability to LC's in neutrally stratified conditions: first in the presence of waves which propagate in the direction of the mean Eulerian velocity (§4) and then opposite to it (§5). The role of stratification is considered in §6 and the results are discussed in §7.

2. Governing equations

2.1. *Background*

We consider the formation of LC's beneath growing or decaying surface waves of characteristic slope $\epsilon \ll 1$ in the presence of stress driven shear in deep water, via a generalization of an initial value problem posed by LP. Here the water is initially at rest and its temperature varies as $T(z)$. At time $t = 0$, surface waves and a stress u_*, due both to the wind and induced viscous action of the waves (see §3.1), are imposed. This stress, which is aligned in a direction we take to be the x-direction, provides the only source of external work, causes the substrate to grow and effects, either directly or indirectly, growth (or decay) of the wave field, which may propagate in either the positive or negative x-direction. The wind on the other hand propagates always in the positive x-direction. Finally, we let the mean free surface coincide with the (x, y) plane and set z positive vertically upwards.

Important parameters are thus u_*, wave frequency σ, streamwise wavenumber α and amplitude a, which together (see below) define a characteristic velocity $\mathcal{V}$, and in combination with the phase velocity, the level of shear, $\mathcal{V}\alpha/\sigma = O(\epsilon^s)$ (see Phillips 1998). Of interest here is the level of shear determined by the phase velocity of the dominant waves in the open ocean, which is $O(\epsilon^{-2})$ larger than $\mathcal{V}$, so $s = 2$ and the waves are irrotational.

The waves interact with themselves (nonlinearly) to yield an $O(\epsilon^2)$ mean drift velocity, the Stokes drift, and the the ensuing $O(\epsilon)$-wave $O(\epsilon^2)$-mean flow interaction is described by the CL or GLM equations (Craik & Leibovich 1976; Andrews & McIntyre 1978). Furthermore the interaction can be unstable to LC's via the CL1 mechanism if the streamwise component of Stokes drift varies spanwise, or CL2 if it does not (Craik 1977). However, in the ocean context where the waves comprise a continuous spectrum of wavenumbers of random phase, it follows that Fourier components in the spanwise y-direction phase mix to zero (Craik & Leibovich 1976), so that CL2 is relevant, and that is the instability mechanism considered here. In this instance the Stokes drift has two non-zero components: $\alpha\sigma a^2 D_1$, which acts in the direction of wave propagation and $u_* a(\sigma/\nu_T)^{\frac{1}{2}} D_3$, which acts in the z-direction; D_3, however, is nonzero only if the waves are temporal (see §3.2).

The perturbation equations may be nondimensionalized in various ways but we follow Leibovich (1977a). In particular we introduce spatial and temporal scales as

$$[(x,\ y,\ z)\alpha^{-1},\ \frac{t}{a\alpha u_*}(\frac{\nu_T}{\sigma})^{\frac{1}{2}}], \tag{2.1}$$

with, since $\mathcal{V} = u_*^2/\alpha\nu_T$, corresponding mean and perturbation velocity components

$$[(U(z,t) + u(y,z,t))\mathcal{V},\ (v(y,z,t),\ w(y,z,t))u_* a(\frac{\sigma}{\nu_T})^{\frac{1}{2}}]. \tag{2.2}$$

Accordingly the temperature perturbation is $\vartheta T'/\alpha$, where prime denotes d/dz and ν_T as an eddy viscosity representative of turbulent diffusivity of momenum. Finally, with streamwise averaged (dimensionless) Eulerian velocity perturbations $\mathbf{u} = (u, v, w)$, unit vectors $(\mathbf{i}, \mathbf{j}, \mathbf{k})$ in (x, y, z) respectively and $\mathrm{D} \equiv \partial/\partial z$, the ensuing perturbation equations relative to the substrate $U(z,t)$ and linear thermocline $T(z)$ are, for temporal waves in $s = 2$ shear (Phillips 1998)

$$\frac{\partial u}{\partial t} + \mathbf{u}\cdot\nabla u = -w\mathrm{D}U - D_3\mathrm{D}u + La\nabla^2 u \tag{2.3a}$$

and

$$\frac{\partial \mho}{\partial t} + \frac{\partial}{\partial y}(\mho v) + \frac{\partial}{\partial z}(\mho w) = -\mathrm{D}(D_3\mho) - \frac{\partial u}{\partial y}\mathrm{D}D_1 + Ri\frac{\partial \vartheta}{\partial y} + La\nabla^2\mho, \tag{2.3b}$$

where

$$\mho = \frac{\partial w}{\partial y} - \frac{\partial v}{\partial z}, \tag{2.3c}$$

with (LP)

$$\frac{\partial \vartheta}{\partial t} + \mathbf{u}\cdot\nabla\vartheta = -w + LaPr^{-1}\nabla^2\vartheta \quad \text{with} \quad \nabla\cdot\mathbf{u} = 0. \tag{2.3d}$$

Here La is the Langmuir number, Pr is a turbulent Prandtl number (where κ_T is the eddy diffusivity of heat) and Ri is a Richardson number, as

$$La = \frac{\alpha\nu_T}{au_*}\left(\frac{\nu_T}{\sigma}\right)^{\frac{1}{2}}, \quad Pr = \frac{\nu_T}{\kappa_T}, \quad Ri = \frac{N^2}{(au_*\alpha)^2(\sigma/\nu_T)},$$

where $N^2 = \beta g T'(z)$ is the Brunt-Väisälä frequency with β the thermal coefficient of expansion and g gravity.

The initial value problem is completed with the boundary conditions

$$\mathbf{k}\cdot\mathbf{u} = \mathrm{D}(\mathbf{u}\times\mathbf{k}) = \vartheta = 0 \quad \text{on} \quad z = 0 \tag{2.4a}$$

$$\mathbf{u}\to 0, \quad \vartheta \to 0 \quad \text{as} \quad z\to-\infty, \tag{2.4b}$$

the initial values

$$\mathbf{u}(\mathbf{x},0) = \mathbf{u}_0(\mathbf{x}), \quad \vartheta(\mathbf{x},0) = 0 \tag{2.4c}$$

and the requirement that $\mathbf{u}_0(\mathbf{x})$ is solinoidal.

2.2. *Numerical formulation*

Prior to proceeding numerically, we rewrite (2.3) in a form that assumes the following: First, that the LC's are spanwise periodic with wavenumber l; and, second, since the substrate is a boundary layer, ensures that the perturbations approach a constant value exponentially fast as $z \to -\infty$ (see Brown & Stewartson 1965; Phillips 1996). We thus write

$$(\mathbf{u}, p, \vartheta) = [\hat{\mathbf{u}}(z,t), \hat{\vartheta}(z,t)]\mathrm{Re}\{\mathrm{e}^{\gamma z + ily}\} \tag{2.5}$$

(where $\gamma \geq 0$ is a constant) and, since the physical domain is semi-infinite, map to the finite plane with the transformation $\zeta = \mathrm{e}^z$, rendering $\mathrm{D} \equiv \zeta\partial/d\zeta$.

We then have

$$\frac{\partial\hat{u}}{\partial t} = -\hat{w}\mathrm{D}U - D_3(\mathrm{D}+\gamma)\hat{u} + La(\mathrm{M}-l^2)\hat{u}, \tag{2.6a}$$

$$(\mathrm{M}-l^2)\frac{\partial\hat{w}}{\partial t} = l^2\hat{u}\mathrm{D}D_1 - \mathrm{D}[D_3(\mathrm{M}-l^2)\hat{w}] + \gamma D_3(\mathrm{M}-l^2)\hat{w} + La(\mathrm{M}-l^2)^2\hat{w} - l^2Ri\hat{\vartheta} \tag{2.6b}$$

and

$$\frac{\partial\hat{\vartheta}}{\partial t} = -\hat{w} + LaPr^{-1}(\mathrm{M}-l^2)\hat{\vartheta} \tag{2.6c}$$

which concur with LP when $D_3 = 0$, albeit with the general operator

$$\mathrm{M} \equiv \zeta\frac{\partial}{\partial\zeta}\left(\zeta\frac{\partial}{\partial\zeta}\right) + 2\gamma\zeta\frac{\partial}{\partial\zeta} + \gamma^2$$

and boundary conditions

$$\frac{\partial\hat{u}}{\partial\zeta} + \gamma\hat{u} = \hat{w} = \frac{\partial^2\hat{w}}{\partial\zeta^2} + (1+2\gamma)\frac{\partial\hat{w}}{\partial\zeta} + \gamma^2 = \hat{\vartheta} = 0 \quad \text{on} \quad \zeta = 1, \tag{2.7a}$$

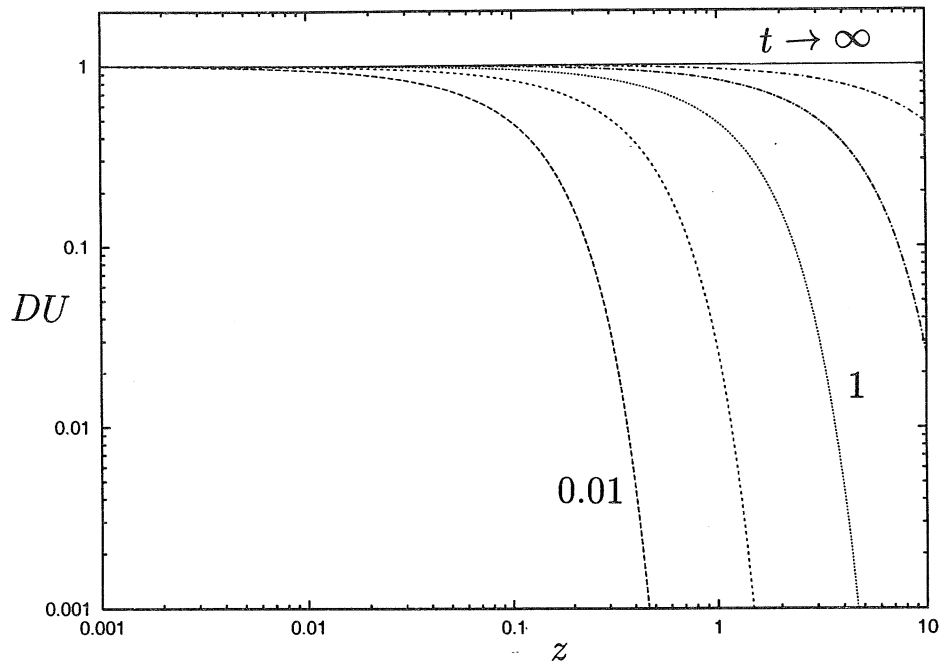

FIGURE 1. Gradients of the Eulerian mean velocity in accelerating laminar flow at $t = 0.01, 0.1, 1.0, 10.0, 100$ and as $t \to \infty$.

$$\text{and} \quad \hat{u} = \hat{w} = \hat{\vartheta} = 0 \quad \text{with all derivatives bounded on} \quad \zeta = 0. \tag{2.7b}$$

LP (with $\gamma = 0$) and Phillips (2000b) with $\gamma = 1$ have solved (2.6) and (2.7) with $D_3 = 0$ numerically. Both employ Galerkin techniques (which LP outline in detail) although Phillips employs various numerical improvements, which are also employed here. In each instance the numerics assume that the transient growth of the substrate, and in this instance the waves, is slow compared with the initial growth of the LC's. This then permits the study of the instability to LC's at snapshots in the time evolution of the substrate and waves.

3. Primary flow

3.1. *Mean shear*

Although LP regard the $O(\epsilon^2)$ mean shear as wind initiated through a wind stress at the surface, it can, as Craik (1982) notes, be just as readily attributed to the free surface boundary condition, *i.e.* by the induced viscous action of the waves (Longuet-Higgins 1953). Specifically, if we suppose that a uniform wave field is rapidly set up at $t = 0$ and that the waves are subsequently maintained at constant amplitude by suitable periodic normal stresses, the analysis of LP remains valid by replacing their wind stress by the velocity gradient determined by the free surface boundary condition. Furthermore, the velocity gradient is likewise determined if the surface is truely free with no applied normal stresses, although here the wave amplitude decays owing to viscous action. Craik further shows that the free surface boundary condition, and thus the component of mean shear caused by it, is greatly affected by surface contamination, but that contamination plays no role in the Stokes drift.

Here we allow for both a wind stress and a free surface wave stress. However, rather than treating

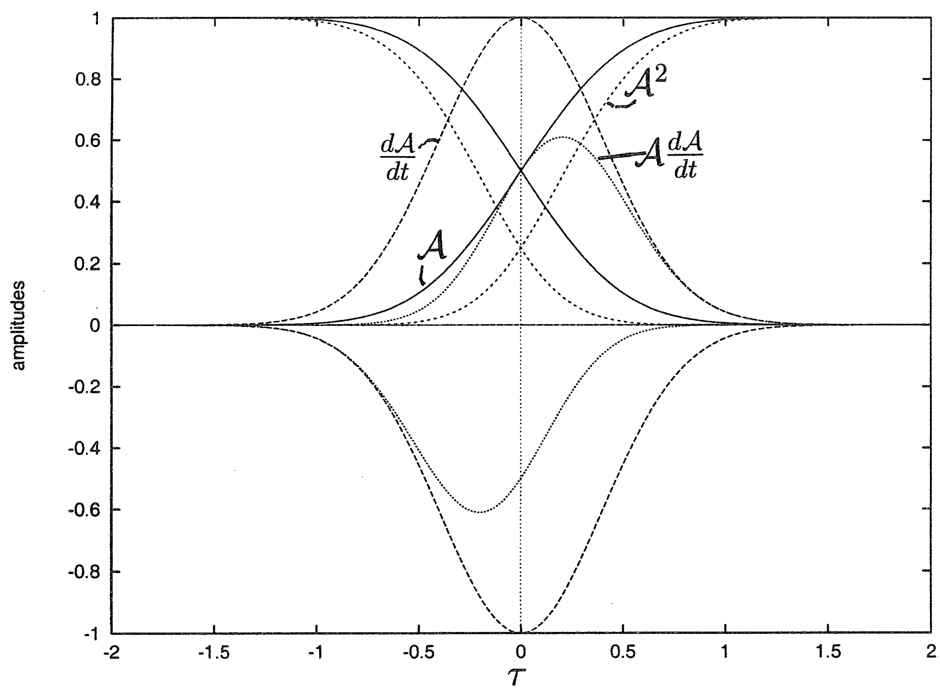

FIGURE 2. Sketch of the amplitude function $\mathcal{A}$ its gradient $d\mathcal{A}/d\tau$ and the products $\mathcal{A}^2$ and $\mathcal{A}d\mathcal{A}/d\tau$ for growing ($n = 1$) and decaying ($n = -1$) waves.

a plethora of cases we choose to employ a consistent set of base flows. Indeed, irrespective of the component values of the wind stress and free surface wave stress, we assume their sum is at all times constant (see §§4, 5). Finally, in order to compare our results with those of LP and Phillips (2000b), we assume the developing substrate shear $\mathrm{D}U(z,t)$ owing to the constant stress u_*, is given always by a solution to the stress Rayleigh problem as

$$\mathrm{D}U = \mathrm{erfc}(\eta) \quad \text{where} \quad \eta = -\frac{z}{2(tLa)^{\frac{1}{2}}}. \tag{3.1}$$

Equation (3.1) is plotted in figure 1 for various values of t, some of which, *viz* $t = 0.01, 1$ and ∞, are used in the examples to follow.

3.2. *Stokes drift*

The simplest example of Stokes drift of relevance here occurs for two dimensional irrotational monochromatic travelling waves of small amplitude, but although D_1 is well known in this instance, that is not the case for D_3. Nevertheless D_3 can be deduced from Craik's (1982b) expressions for the generalized Stokes drift for monochromatic rotational waves or Phillips' (2001a) counterparts for broad spectrums of temporal rotational waves. Both reduce, for two-dimensional irrotational monochromatic waves, to

$$D_1 = b\mathcal{A}^2(\tau)\mathrm{e}^{2z} \quad \text{and} \quad D_3 = b\mathcal{A}(\tau)\frac{d\mathcal{A}}{d\tau}\mathrm{e}^{2z} \quad (-\infty < z \leq 0), \tag{3.2}$$

where $\tau + \tau_0 = t$, τ_0 is an offset and b is positive constant we set equal to 2 to concur with LP and Phillips (2000b).

Note that in writing (3.2), we have interpreted a (in our scaling in §2.1) as the maximum amplitude of the waves and depict modulations to that amplitude by $a\mathcal{A}(\tau)$, where $\mathcal{A}(\tau) \in [0, 1]$. Observe too

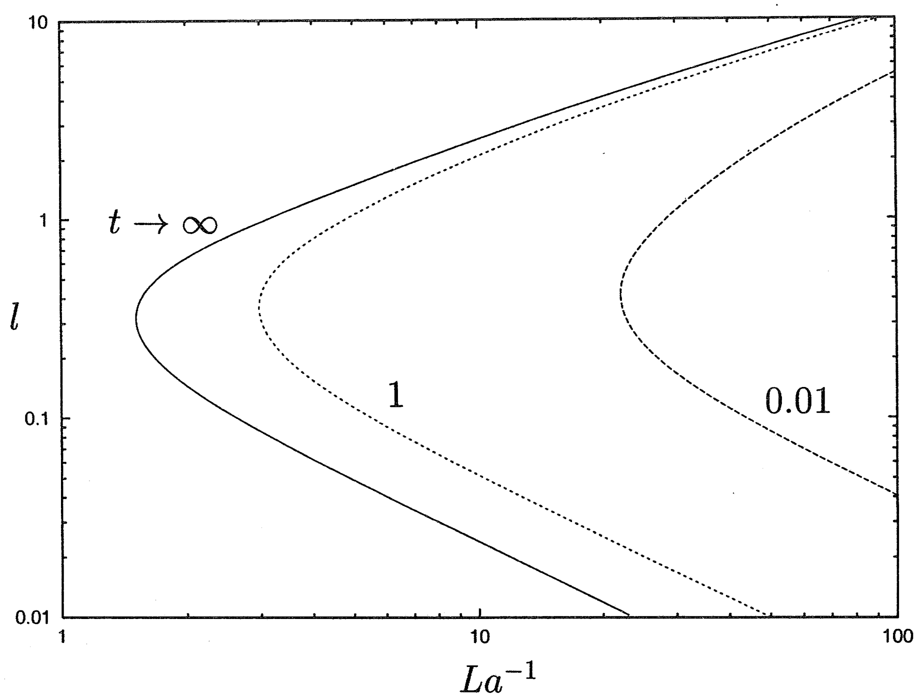

FIGURE 3. Neutral curves for developing shear at $t = 0.01, 1$ and $t \to \infty$ in the presence of neutral waves.

that D_1 is nonzero for all nonzero $\mathcal{A}$, while D_3 is nonzero only if the waves are temporal. We do not solve for $\mathcal{A}(\tau)$, however; rather we assume it takes the form

$$\mathcal{A}(\tau) = \frac{1}{2}\left[2 - n^2 + n\mathrm{erf}(B\tau)\right] \tag{3.3}$$

where $n = [1, 0, -1]$, according to whether the waves are growing, neutral or decaying.

For convenience we set $B = \sqrt{\pi}$, so that $\mathrm{erf}(B) \approx 0.99$. Then for growing waves we see that $D_3 \approx 0$ when $\tau = -1$ while D_3 is a maximum near $\tau = 0.2$; likewise $D_3 \approx D_1$ when $\tau = 0.3$, while $D_1 \approx 2D_3$ when $\tau = 0.5$. Finally, although $D_1(-.5) \approx 0$, we see that $D_3(-.5)$ while small is much greater than $D_1(-.5)$. Similar cases exist for decaying waves, albeit with $D_3(\tau)$ replaced by $-D_3(-\tau)$, and so test cases were done at $\tau = 0, \pm0.2, \pm0.3, \pm0.5, \pm1$. Curves of $\mathcal{A}$, $\mathcal{A}^2$ and $\mathcal{A}d\mathcal{A}/d\tau$ are plotted in figure 2.

3.3. *Time scales*

In Melville *et al* 's (1998) experiments of the formation of LC's in wind driven $s = 0$ shear, the substrate, waves and LC's grow on the same time scale. In $s = 2$ shear, however, wave and substrate growth are slow compared with the initial exponential evolution of the LC's. Indeed from the viewpoint of the instability, the substrate and wave field are essentially frozen, which permits us to consider the instability at various independent stages of evolution of the substrate and waves specified by the offset τ_0. In consequence we investigate cases at the specific values of t and τ given earlier; each is discussed in §4.

4. Aligned wind and waves

We begin by considering flows in which the wind and waves propagate in the same direction. And, since external work accomplished by the application of suitable stresses, is required to maintain

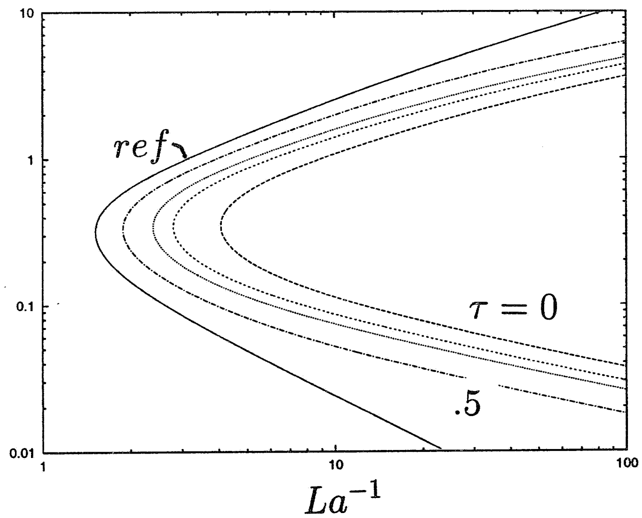

FIGURE 4. Developed shear with growing waves. Neutral curves for $t \to \infty$ with $\tau = 0, .2, .3, .5$.

purely periodic waves in a viscous liquid, we take the view that the waves are neutral or grow only in the presence of a wind stress, and decay only in the absence of a wind stress. Then, in order to compared various cases, we require, as mentioned in §3.1, that the sum of the wind and free surface wave stresses, remains constant. Rather than specify proportions of each stress, however, we instead specify values of τ and t. This then permits us to consider and compare several credible scenarios, beginning with the case of developing shear in the presence of neutral waves. In all cases the flow is non-stratified (*i.e.* $Ri = 0$).

4.1. *Developing shear with neutral waves*

Here the waves reach maturity well before the substrate, so we let $\tau \to \infty$ and consider three values of t, *viz* 0.01, 1 and ∞, as shown in figure 3. This case was first investigated by LP who found, in accord with figure 3, that the least stable situation occurs in the limit $t \to \infty$. Physically this means that the full extent of the developing LC's are subjected to uniform shear. Phillips (2001b) further determined that the $\tau, t \to \infty$ curve depicts the least stable neutral curve for the double limit $Pr = Ri = 0$, so we use it as a reference in the cases to follow. Note too that onset in the reference case occurs at $l_{c0} = 0.3187$ and $La_{c0}^{-1} = 1.5157$.

4.2. *Developed shear with growing waves*

We now consider the reverse case, in which the substrate reaches maturity prior to the waves. Here then the shear is uniform while the waves continue to grow. Neutral curves for this case are plotted in figure 4 along with the reference curve, which of course is recovered, as (see figure 2) $\tau \to \infty$. Of particular interest is the case for which D_3 is a maximum ($\tau = 0.2$) which falls to the right of the reference curve. This indicates that growing waves in the presence of uniform shear are stabilizing to the generation of LC's. In fact of the cases with growing waves considered, the least stable is that for $\tau = 0.5$ (at which point $D_1 \approx 2D_3$). Note too that the spanwise wavenumber at onset at $\tau = 0.5$ is $l_c = .3320$; thus since $l_c > l_{c0}$ we infer that growing waves act to increase the onset spanwise wavenumber.

4.3. *Developed shear with decaying waves*

Of course if after some time the wind were to suddenly diminish, the waves may also decay in the presence of uniform shear. In this instance, as we see in figure 5, the flow is stabilizing to LC's for $l \gg l_{c0}$ and destabilizing for $l \ll l_{c0}$. Note, however, that La_c^{-1} at all times exceeds the

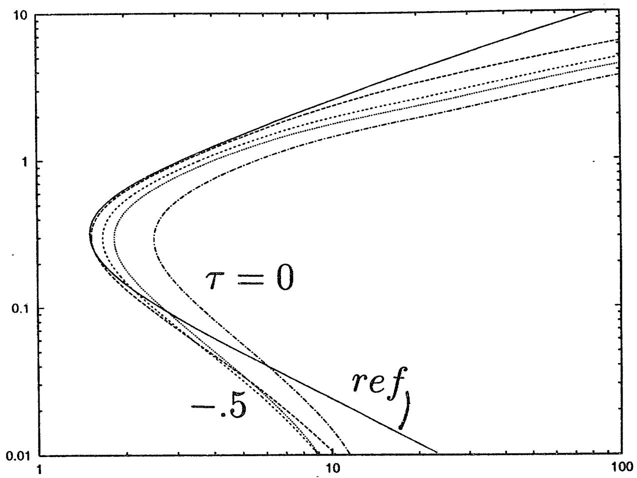

FIGURE 5. Developed shear with decaying waves. Neutral curve for $t \to \infty$ with $\tau = -.5, -.3, -.2, 0$.

global lowerbound of 1.4395 for stably stratified flow reported by LP. The interaction is also slightly stabilizing at onset for $\tau = -0.5$, where, compared with La_{c0}^{-1}, we have $La_c^{-1} = 1.5418$. Furthermore $l_c = .3063$ here, suggesting that decaying waves act to decrease the spanwise wavenumber at onset. Finally, we note that contrary the above cases for growing or neutral waves, which are unstable only for wavenumbers $l > 0$, the case with decaying waves is unstable even in the limit (not shown) $l \to 0$, albeit at $La_c^{-1} \gg La_{c0}^{-1}$.

4.4. *Developing shear with growing waves.*

We turn now to the case in which the shear and waves grow at comparable rates. Interestingly, although the interaction is stable to the formation of LC's when $t = 0.01$ for $\tau \in [-1, 0.5]$, it is unstable to LC's at $\tau = 1$, as we see in figure 6. Since $D_1 \gg D_3$ when $\tau = 1$ it is evident that the stabilizing effect of growing waves (through D_3) can be overcome by D_1 to drive the instability, even when the shear layer is thin (*i.e.* the e-folding depth is $\ll 1$). Note, however, that LC's form only for spanwise wavenumbers larger than l_{c0}, and thus that there is a long wave cutoff.

For more developed shear on the other hand, *i.e.* $t = 1$, the flow is unstable to LC's at all τ, albeit for a restricted range of l; this case is shown in figure 7. Here, in accord with our ealier findings for growing waves, the flow the stabilizing to the formation of LC's and onset occurs at spanwise wavenumbers in excess of l_{c0}.

4.5. *Developing shear with decaying waves*

On the other hand developing shear, which can occur in the absence of wind owing to the wave induced surface stress and decaying waves, is unstable to LC's for all τ considered at both $t = 0.01$ and $t = 1$, as we see in figures 8 and 9. But comparison of these figures with figure 5, shows that developing shear is stabilizing to the formation of LC's, at least for $l > 0.05$. Not surprizingly the case $t \to \infty$ is the least, and $t = 0.01$ the most, stabilizing, with the implication that the flow is stable to the formation of LC's in the limit $t \to 0$, *i.e.* in the absence of shear, as it must be.

5. Opposed wind and waves

We now consider the situation in which the wind and waves propogate in opposite directions. Of course their respective stresses are also opposite but their sum, as before, is constant. Thus, since u_* is by definition aligned in the x-direction, the magnitude of the wind stress must necessarily exceed

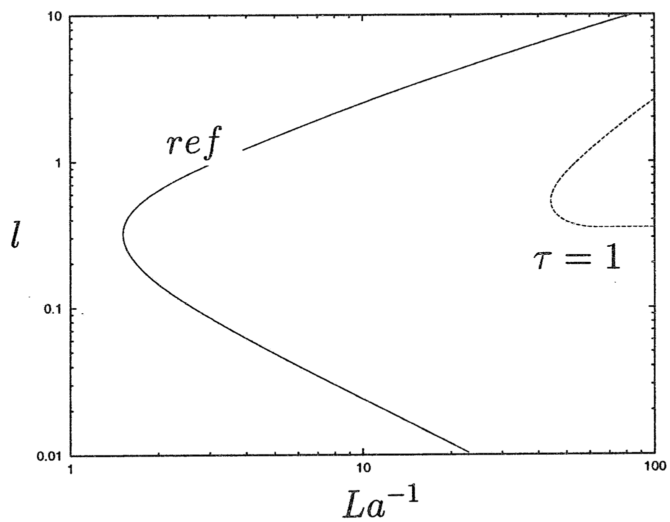

FIGURE 6. Developing shear with growing waves for $t = 0.01$ and $\tau = 1$. Note that the flow is stable to the formation of LC's for $\tau \in [-1, 0.5]$.

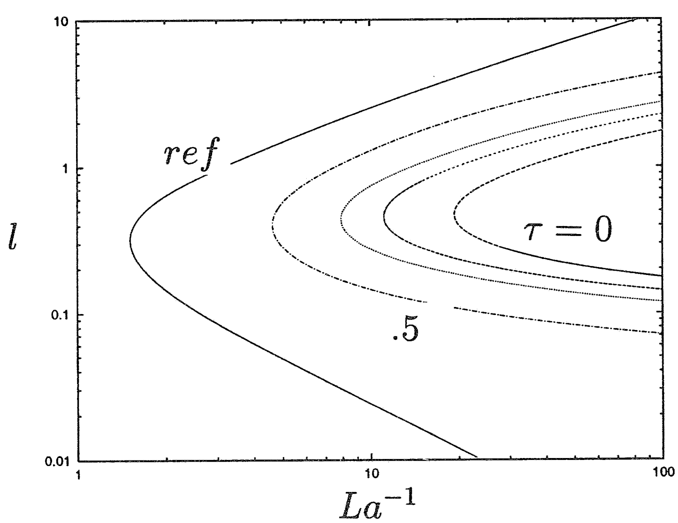

FIGURE 7. Developing shear with growing waves. for $t = 1$ and $\tau = 0, .2, .3, .5$.

the magnitude of the free surface wave stress, so that the mean Eulerian shear flow is always counter to the streamwise component of Stokes drift. Decaying waves are therefore physically intuitive and, interestingly, we find the flow is unstable to LC's *only* if the waves are decaying, as we see in §5.1, 5.2. Here the substrate is also neutrally stratified (so $Ri = 0$).

5.1. *Developed shear with decaying waves*

We look first at figure 10 and observe that the flow is least stable when $\tau = -0.3$, at which point $D_1 \approx -D_3$. Observe too that the neutral curves are vastly different from the single albow form of their coflowing counterparts. Rather the neutral curves are here fingered, with bands of l that are unstable to LC's and bands that are stable. Notice though, that the bands blend into each other as the waves evolve with τ.

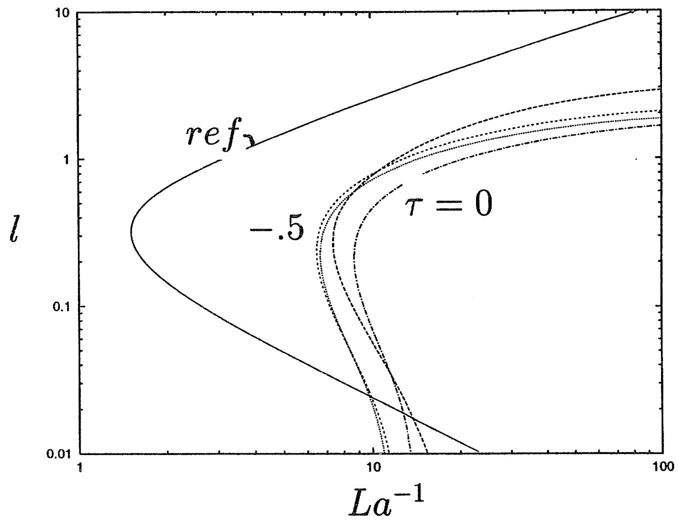

FIGURE 8. Developing shear with decaying waves. for $t = 0.01$ with $\tau = -.5, -.3, -.2, 0$.

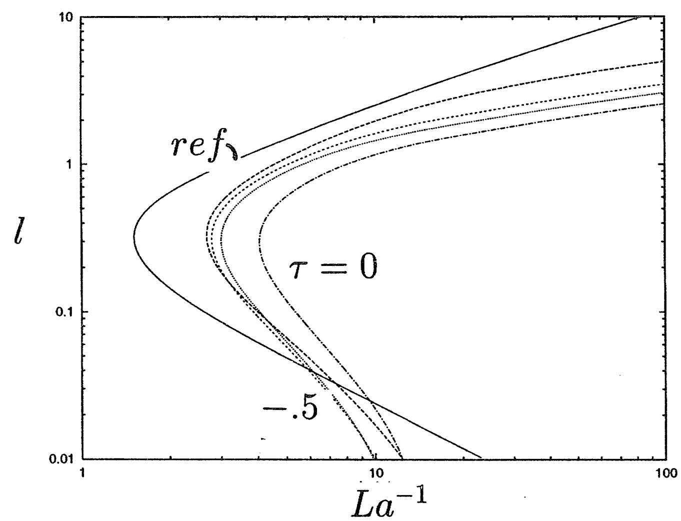

FIGURE 9. Developing shear with decaying waves. for $t = 1$ with $\tau = -.5, -.3, -.2, 0$.

5.2. *Developing shear with decaying waves*

Much the same features occur as the substrate grows, although, in accord with our earlier findings, the case with fully developed shear is the least stable, as we see by comparing figures 10, 11 and 12. Also evident is a region of instability for $l \ll 1$. This is the least stable finger and continues to the long wave limit $l \to 0$; this finger is in fact also present but outside the plotted range in the fully developed case.

6. The role of stratification

Phillips (2001b) considers the formation of LC's in the presence of neutral waves and stratification over a wide range of Pr and Ri numbers. Our intent here is to ascertain the role of stratification on the instability in the presence of temporal waves. However, in view of the wide parameter range, we choose representative values of Prandtl and Richardson numbers, $Pr = 6.7$ and $Ri = \pm 0.1$ say, and

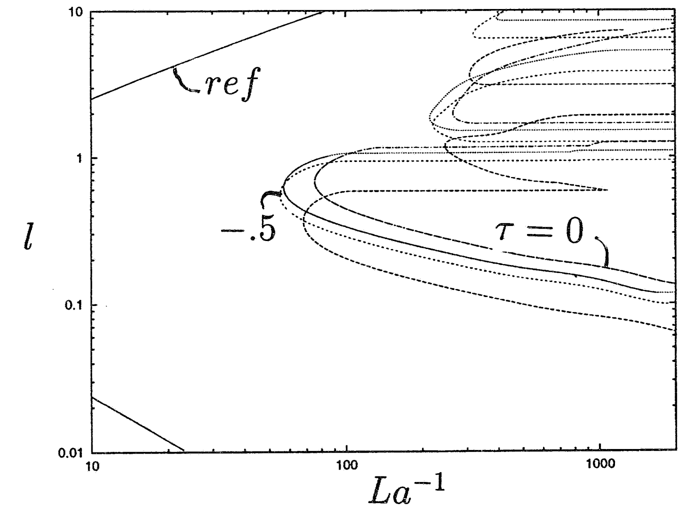

FIGURE 10. Developed shear with opposed decaying waves. Neutral curve for $\tau = -.5, -.3, -.2, 0$.

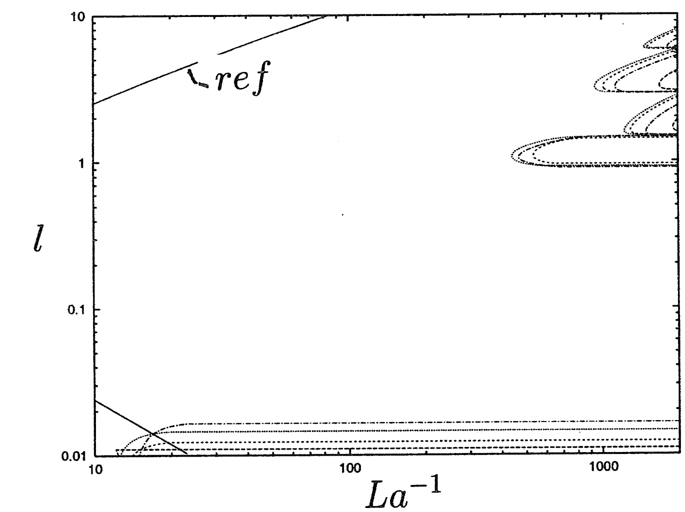

FIGURE 11. Developing shear with opposed decaying waves. Neutral curve for $\tau = -.5, -.3, -.2, 0.$ in shear time: $t = 0.01$.

further choose the least stable base flow ($t \to \infty$) and the least stable case for growing ($\tau = 0.5$) and decaying ($\tau = -0.5$) waves. These are plotted in figures 14, 15 and 16.

6.1. *Aligned wind and waves*

First, we find that growing waves aligned with the wind in the presence of stable stratification ($Ri > 0$) are stable to the formation of LC's, while neutral and decaying waves are unstable to LC's. Furthermore while both cases are stabilizing relative to the reference case, decaying waves are destabilizing relative to neutral waves, at least for $l < 1$, as we see in figure 13. Note too that the curve for the decaying wave case depicts a fingered pattern reminicent of its counterparts in §5, although here the fingers are connected.

On the other hand growing, neutral and decaying waves are unstable to the formation of LC's in unstably stratified flow ($Ri < 0$) and destabilizing relative to the reference flow, as we see in

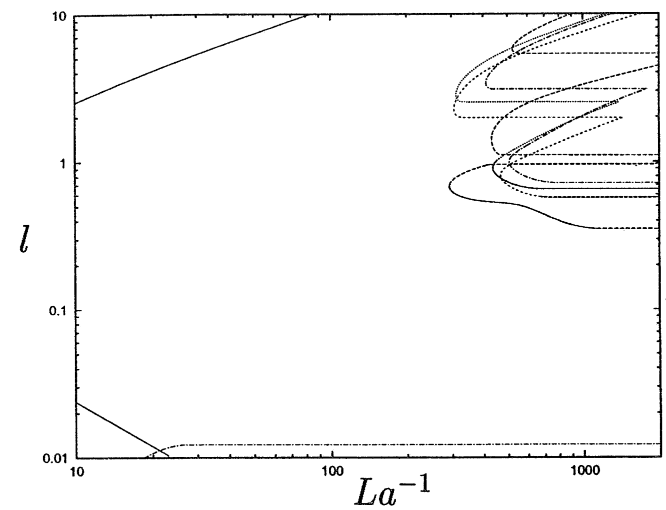

FIGURE 12. Developing shear with opposed decaying waves. Neutral curve for $\tau = -.5, -.3, -.2, 0.$ in shear time: $t = 1$.

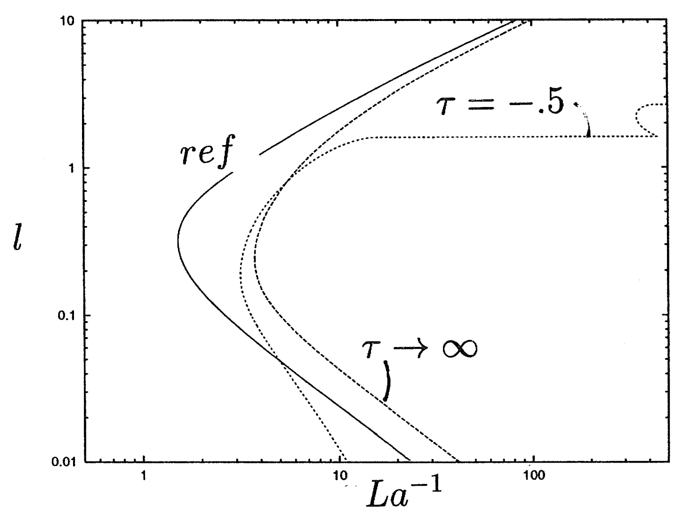

FIGURE 13. Developed stably stratified shear with neutral and decaying waves for $Ri = 0.1$ and $Pr = 6.7$; Note that this configuration is stable to growing waves. Neutral curves for $t \to \infty$ with $\tau = -.5$.

figure 14. Moreover, in accord with our earlier findings, decaying waves are destabilizing, at least for $l < 0.1$, and growing waves stabilizing, relative to the neutral waves case.

6.2. *Opposed wind and waves*

When the wind and waves are opposed, however, and the flow is stably stratified, only decaying waves are destabilizing to LC's, as we see in figure 15. When the flow is unstably stratified, on the other hand, all waves are destabilizing to LC's. Note, however, that in this instance growing waves are destabilizing and decaying waves stabilizing relative to the neutral wave case. Furthermore, decaying waves depict a long wave cut-off, as we see in figure 16.

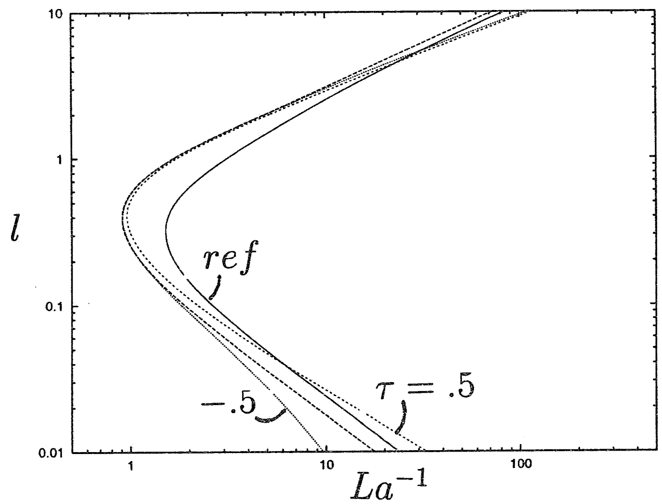

FIGURE 14. Developed unstably stratified shear with growing, neutral and decaying waves for $Ri = -0.1$ and $Pr = 6.7$. Neutral curves for $t \to \infty$ with $\tau = \pm.5$.

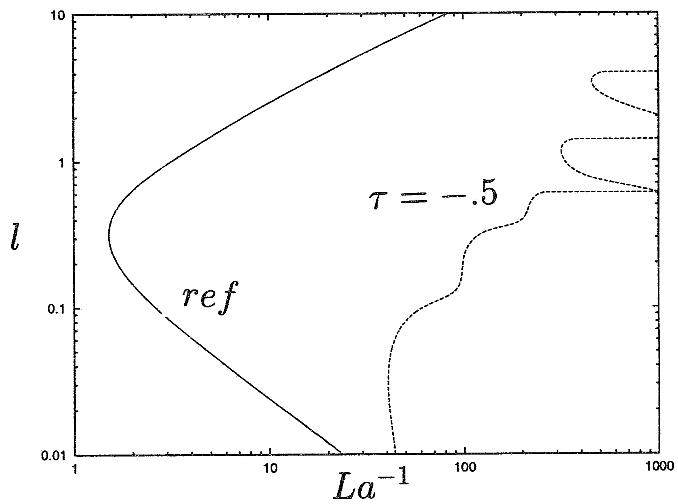

FIGURE 15. Developed stably stratified shear with opposed decaying waves for $Ri = 0.1$ and $Pr = 6.7$; Note that this configuration is stable to neutral and growing waves. Neutral curves for $t \to \infty$ with $\tau = -.5$.

7. Discussion

Craik (1982c) gives a simple kinematical explanation of CL2 in inviscid flow: specifically that the Stokes drift gradient $\mathrm{D}D_1$ causes vortex lines to tilt forward wherever the Eulerian mean shear is laterally distorted, giving rise to a longitudinal component of vorticity and ultimately vortices. Here we find that temporal waves, through the gradient $\mathrm{D}D_3$, act to further advect vortex lines, but up or down according to whether the waves are growing or decaying, thereby increasing or decreasing the z-gradient of streamwise vorticity and, in turn, the rate at which the instability grows.

To further pursue this point, we return to (2.3b) and the term $\mathrm{D}(D_3\mho)$ which depicts, as noted above, the advection of $\mho$ in z owing to D_3. To determine the role of $\mathrm{D}(D_3\mho)$ on the instability, however, we expand it and note that of the components that arise, the key one is $-\partial w/\partial y \mathrm{D}D_3$ which acts to counter or reinforce the forcing term in CL2, *viz* $-\partial u/\partial y \mathrm{D}D_1$. In particular, while the

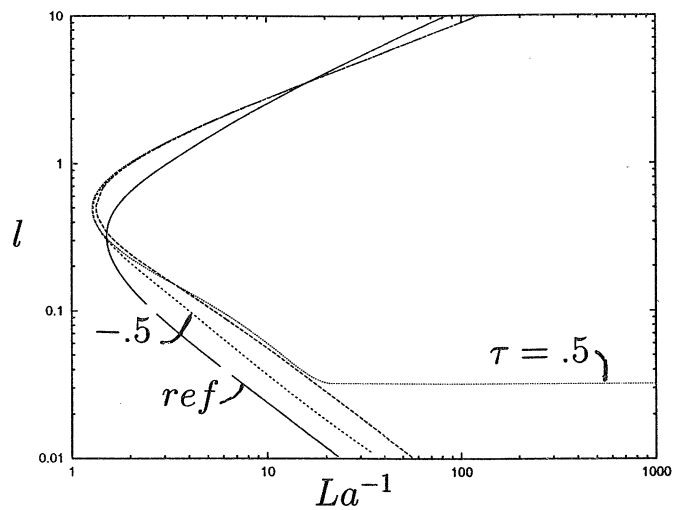

FIGURE 16. Developed unstably stratified shear with opposed neutral and decaying waves for $Ri = -0.1$ and $Pr = 6.7$. Neutral curves for $t \to \infty$ with $\tau = \pm.5$.

velocity components u and w are in phase but of opposite sign always, the Stokes drift components D_1 and D_3 have the same sign only when the waves grow.

We could therefore have anticipated that growing waves are stabilizing and decaying waves destabilizing to LC's. But we could not have anticipated the details, for example the result that destabilization to LC's in decaying waves pertains only to wavenumbers $l \ll 1$.

This work was supported by the National Science Foundation through grants OCE-9696161 and OCE-9818092.

REFERENCES

ANDREWS, D. G. & MCINTYRE, M. E. 1978 An exact theory of nonlinear waves on a Lagrangian-mean flow. *J. Fluid Mech.*, **89**, 609–646.

BROWN, S.N. & STEWARTSON. K 1969 Laminar Separation *Ann. Rev. Fluid Mech.* **1**, 45-72.

COX, S. M., LEIBOVICH, S., MOROZ, I. M. & TANDON, A. 1992 Non-linear dynamics in Langmuir circulations with $O(2)$ symmetry. *J. Fluid Mech.*, **241**, 669-704.

COX, S. M. & LEIBOVICH, S. 1993 Langmuir circulations in a surface layer bounded by a strong thermocline. *J. Phys. Oceanogr.* **23** 1330-1345.

COX, S. M. & LEIBOVICH, S. 1997 Large-scale three-dimensional Langmuir circulation *Phys. Fluids* **9** 2851-2863.

CRAIK, A. D. D. 1977 The generation of Langmuir circulations by an instability mechanism, *J. Fluid Mech.*, **81**, 209-223.

CRAIK, A.D.D. 1982a The drift velocity of water waves. *J. Fluid Mech.*, **116**, 187-205.

CRAIK, A.D.D. 1982b The generalized Lagrangian-mean equations and hydrodynamic stability. *J. Fluid Mech.*, **125**, 27-35.

CRAIK, A.D.D. 1982c Wave-induced longitudinal-vortex instability in shear layers. *J. Fluid Mech.*, **125**, 37-52.

CRAIK, A.D.D., AND LEIBOVICH, S. 1976 A rational model for Langmuir circulations, *J. Fluid Mech.*, **73**, 401-426.

DRAZIN, P.G. AND HOWARD, L.N. 1966 Hyrodynamic instability of parallel flow in inviscid fluid. In *Advances in applied mechanics*, vol 7 ed. G. Kuerti, pp 1-89. New York, Academic Press.

DRAZIN, P.G. AND REID, W.H. 1981 *Hydrodynamic Stability* Cambridge University Press.

GARGETT, A. E. 1989 Ocean turbulence *Ann. Rev. Fluid Mech.*, **21**, 419-451.

FOSTER, T.D. 1965 Stability of homogeneous fluid cooled uniformly from above. *Phys. Fluids*, **8**, 1249-1257.

HOMSY, G.M. 1973 Global stability of time dependent flows: impulsively heated or cooled liquid layers. *J. Fluid Mech.*, **60**, 129-139.

KENNEY, B. C. 1993 Observations of coherent bands of algae in a surface shear layer. *Limnol. Oceanogr.*, **38**, 1059-1067.

LANGMUIR, I 1938 Surface motion of water induced by wind. *Science*, **87**, 119-123.

LEIBOVICH, S, 1977a Convective instability of stably stratified water in the ocean. *J. Fluid Mech.*, **82**, 561-585.

LEIBOVICH, S, 1977b On the evolution of the system of wind drift currents and Langmuir circulations in the ocean. Part 1. Theory and averaged current. *J. Fluid Mech.*, **79**, 715-743.

LEIBOVICH, S, 1980 On wave-current interaction theories of Langmuir circulations. *J. Fluid Mech.*, **99**, 715-724.

LEIBOVICH, S, 1983 The form and dynamics of Langmuir circulations, *Ann. Rev. Fluid Mech.*, **15**, 391-427.

LEIBOVICH, S AND PAOLUCCI, S 1980 Energy stability of the Eulearian-mean motion in the upper ocean to three-dimensional perturbations *Phys. Fluids*, **23**, 1286-1290.

LEIBOVICH, S & PAOLUCCI, S. 1981 The instability of the ocean to Langmuir circulations. *J. Fluid Mech.*, **102**, 141-167.

LEIBOVICH, S., LELE, S. & MOROZ, I. M. 1989 Nonlinear dynamics in Langmuir circulations and thermosolutal convection. *J. Fluid Mech.*, **198**, 471-511.

LI, M. & GARRETT, C. 1993 Cell merging and the jet/downwelling ratio in Langmuir circulation *J. Mar. Res.*, **51**, 737-769.

LI, M. & GARRETT, C. 1997 Mixed layer deepening due to Langmuir circulation. *J. Phys. Ocean..*, **27**, 121-132.

LI, M., ZAHARIEV, K. & GARRETT, C. 1995 Role of Langmuir circulation in the deepening of the ocean surface mixed layer. *Science*, **270**, 1955-1957.

LONGUET-HIGGINS, M.S., 1953 Mass transport in water waves. *Phil. Trans. R. Soc. Lond.* A, **245**, 535-581.

MCWILLIAMS, J.C., SULLIVAN, P.P. & MOENG, C-H. 1997 Langmuir circulations in the ocean. *J. Fluid Mech.* **334**, 1-30.

MELVILLE, W.K., SHEAR, R. & VERON, F. 1998 Laboratory measurements of the generation and evolution of Langmuir circulations. *J. Fluid Mech.* **364**, 31-58.

PHILLIPS, W.R.C. 1996 On a class of unsteady boundary layers of finite extent *J. Fluid Mech.*, **319**, 151-170.

PHILLIPS, W.R.C. 1998 Finite amplitude rotational waves in viscous shear flows. *Stud. Appl. Math*, **101**, 23-47.

PHILLIPS, W.R.C. 2000 Eulerian space-time correlations in turbulent shear flows. *Phys. Fluids*, **12**, 2056-2064.

PHILLIPS, W.R.C. 2001a On the pseudomomentum and generalized Stokes drift in a spectrum of rotational waves. *J. Fluid Mech.*, (to appear)

PHILLIPS, W.R.C. 2001b On an instability to Langmuir circulations and the role of Prandtl and Richardson numbers. *J. Fluid Mech.*, (submitted)

PLUEDDEMANN, A.J., SMITH, J.A., FARMER, D.M., WELLER, R.A., CRAWFORD, W.R., PINKEL, R., VAGLE, S. & GNANADESIKAN, A. 1996 Structure and variability of Langmuir circulation during the Surface Waves Processes Program. *J. Geophys. Res.*, **101**, 3525-3543.

PLUEDDEMANN, A.J., WELLER, R.A. 1999 Structure and evolution of the oceanic surface boundary layer during the Surface WAves Processes Program. *J. Marine Syst.*' **21**, 85-102.

SKYLLINGSTAD, E.D. & DENBO, D.W. 1995 An ocean large eddy simulation of Langmuir cells and convection in the surface mixed layer. *J. Geophys. Res.* **100**, 8501-8522.

SMITH, J.A. 1992 Observed growth of Langmuir circulation *J. Geophys. Res.* **97**, 5651-5664.

SMITH, J.A. 1998 Evolution of Langmuir circulation in a storm *J. Geophys. Res.* **103**, 12649-12668.

SMITH, J., PINKEL, R. & WELLER, R. A. 1987 Velocity structure in the mixed layer during MILDEX. *J. Phys. Oceanogr*, **17**, 425-439.

THORPE, S. A. & HALL, A. J. 1982 Observations of the thermal structure of Langmuir circulation. *J. Fluid Mech.*, **114**, 237-250.

WELLER, R. A., DEAN, J. P., MARRA, J., PRICE, J. F., FRANCIS, E. A. & BROADMAN, D. C.

1985 Three-dimensional flow in the upper ocean *Science*, **227**, 1552-1556.
WELLER, R. A. & PRICE, J. F. 1988 Langmuir circulation within the oceanic mixed layer *Deep-Sea Res.* **35**, 711-747.
WELLER, R. A. & PLUEDDEMANN, A.J 1996 Observations of the vertical structure of the oceanic boundary layer. *J. Geophys. Res-Oceans*, **101**, 3525-3543.
ZEDEL, L. & FARMER, D. 1991 Organized structures in subsurface bubble clouds: Langmuir circulation in the upper ocean. *J. Geophys. Res.*, **96**, 8889-8900.

List of Recent TAM Reports

No.	Authors	Title	Date
876	Stremler, M. A., and H. Aref	Motion of three point vortices in a periodic parallelogram—*Journal of Fluid Mechanics* **392**, 101-128 (1999)	Feb. 1998
877	Dey, N., K. J. Hsia, and D. F. Socie	On the stress dependence of high-temperature static fatigue life of ceramics	Feb. 1998
878	Brown, E. N., and N. R. Sottos	Thermoelastic properties of plain weave composites for multilayer circuit board applications	Feb. 1998
879	Riahi, D. N.	On the effect of a corrugated boundary on convective motion—*Journal of Theoretical and Applied Mechanics* **29**, 22–36 (2000)	Feb. 1998
880	Riahi, D. N.	On a turbulent boundary layer flow over a moving wavy wall	Mar. 1998
881	Riahi, D. N.	Vortex formation and stability analysis for shear flows over combined spatially and temporally structured walls—*Mathematical Problems in Engineering* **5**, 317–328 (1999)	June 1998
882	Short, M., and D. S. Stewart	The multi-dimensional stability of weak heat release detonations—*Journal of Fluid Mechanics* **382**, 109–135 (1999)	June 1998
883	Fried, E., and M. E. Gurtin	Coherent solid-state phase transitions with atomic diffusion: A thermomechanical treatment—*Journal of Statistical Physics* **95**, 1361–1427 (1999)	June 1998
884	Langford, J. A., and R. D. Moser	Optimal large-eddy simulation formulations for isotropic turbulence—*Journal of Fluid Mechanics* **398**, 321–346 (1999)	July 1998
885	Riahi, D. N.	Boundary-layer theory of magnetohydrodynamic turbulent convection—*Proceedings of the Indian National Academy (Physical Science)* **65A**, 109–116 (1999)	Aug. 1998
886	Riahi, D. N.	Nonlinear thermal instability in spherical shells—in *Nonlinear Instability, Chaos and Turbulence* **2**, 377–402 (1999)	Aug. 1998
887	Riahi, D. N.	Effects of rotation on fully non-axisymmetric chimney convection during alloy solidification—*Journal of Crystal Growth* **204**, 382–394 (1999)	Sept. 1998
888	Fried, E., and S. Sellers	The Debye theory of rotary diffusion—*Archive for Rational Mechanics and Analysis*, in press (2000)	Sept. 1998
889	Short, M., A. K. Kapila, and J. J. Quirk	The hydrodynamic mechanisms of pulsating detonation wave instability—*Proceedings of the Royal Society of London, A* **357**, 3621–3638 (1999)	Sept. 1998
890	Stewart, D. S.	The shock dynamics of multidimensional condensed and gas phase detonations—Proceedings of the 27th International Symposium on Combustion (Boulder, Colo.)	Sept. 1998
891	Kim, K. C., and R. J. Adrian	Very large-scale motion in the outer layer—*Physics of Fluids* **2**, 417–422 (1999)	Oct. 1998
892	Fujisawa, N., and R. J. Adrian	Three-dimensional temperature measurement in turbulent thermal convection by extended range scanning liquid crystal thermometry—*Journal of Visualization* **1**, 355–364 (1999)	Oct. 1998
893	Shen, A. Q., E. Fried, and S. T. Thoroddsen	Is segregation-by-particle-type a generic mechanism underlying finger formation at fronts of flowing granular media?—*Particulate Science and Technology* **17**, 141–148 (1999)	Oct. 1998
894	Shen, A. Q.	Mathematical and analog modeling of lava dome growth	Oct. 1998
895	Buckmaster, J. D., and M. Short	Cellular instabilities, sub-limit structures, and edge-flames in premixed counterflows—*Combustion Theory and Modeling* **3**, 199–214 (1999)	Oct. 1998
896	Harris, J. G.	*Elastic waves*—Part of a book to be published by Cambridge University Press	Dec. 1998
897	Paris, A. J., and G. A. Costello	Cord composite cylindrical shells	Dec. 1998
898	Students in TAM 293–294	Thirty-fourth student symposium on engineering mechanics (May 1997), J. W. Phillips, coordinator: Selected senior projects by M. R. Bracki, A. K. Davis, J. A. (Myers) Hommema, and P. D. Pattillo	Dec. 1998

List of Recent TAM Reports (cont'd)

No.	Authors	Title	Date
899	Taha, A., and P. Sofronis	A micromechanics approach to the study of hydrogen transport and embrittlement	Jan. 1999
900	Ferney, B. D., and K. J. Hsia	The influence of multiple slip systems on the brittle–ductile transition in silicon—*Materials Science Engineering A* **272**, 422–430 (1999)	Feb. 1999
901	Fried, E., and A. Q. Shen	Supplemental relations at a phase interface across which the velocity and temperature jump—*Continuum Mechanics and Thermodynamics* **11**, 277–296 (1999)	Mar. 1999
902	Paris, A. J., and G. A. Costello	Cord composite cylindrical shells: Multiple layers of cords at various angles to the shell axis	Apr. 1999
903	Ferney, B. D., M. R. DeVary, K. J. Hsia, and A. Needleman	Oscillatory crack growth in glass—*Scripta Materialia* **41**, 275–281 (1999)	Apr. 1999
904	Fried, E., and S. Sellers	Microforces and the theory of solute transport—*Zeitschrift für angewandte Mathematik und Physik* **51**, 732–751 (2000)	Apr. 1999
905	Balachandar, S., J. D. Buckmaster, and M. Short	The generation of axial vorticity in solid-propellant rocket-motor flows	May 1999
906	Aref, H., and D. L. Vainchtein	The equation of state of a foam—*Physics of Fluids* **12**, 23–28 (2000)	May 1999
907	Subramanian, S. J., and P. Sofronis	Modeling of the interaction between densification mechanisms in powder compaction	May 1999
908	Aref, H., and M. A. Stremler	Four-vortex motion with zero total circulation and impulse—*Physics of Fluids* **11**, 3704-3715	May 1999
909	Adrian, R. J., K. T. Christensen, and Z.-C. Liu	On the analysis and interpretation of turbulent velocity fields—*Experiments in Fluids* **29**, 275–290 (2000)	May 1999
910	Fried, E., and S. Sellers	Theory for atomic diffusion on fixed and deformable crystal lattices—*Journal of Elasticity*, in press (2000)	June 1999
911	Sofronis, P., and N. Aravas	Hydrogen induced shear localization of the plastic flow in metals and alloys	June 1999
912	Anderson, D. R., D. E. Carlson, and E. Fried	A continuum-mechanical theory for nematic elastomers—*Journal of Elasticity* **56**, 33–58 (1999)	June 1999
913	Riahi, D. N.	High Rayleigh number convection in a rotating melt during alloy solidification—*Recent Developments in Crystal Growth Research* **2**, 211–222 (2000)	July 1999
914	Riahi, D. N.	Buoyancy driven flow in a rotating low Prandtl number melt during alloy solidification—*Current Topics in Crystal Growth Research*, in press (2000)	July 1999
915	Adrian, R. J.	On the physical space equation for large-eddy simulation of inhomogeneous turbulence	July 1999
916	Riahi, D. N.	Wave and vortex generation and interaction in turbulent channel flow between wavy boundaries	July 1999
917	Boyland, P. L., M. A. Stremler, and H. Aref	Topological fluid mechanics of point vortex motions	July 1999
918	Riahi, D. N.	Effects of a vertical magnetic field on chimney convection in a mushy layer—*Journal of Crystal Growth* **216**, 501–511 (2000)	Aug. 1999
919	Riahi, D. N.	Boundary mode–vortex interaction in turbulent channel flow over a non-wavy rough wall	Sept. 1999
920	Block, G. I., J. G. Harris, and T. Hayat	Measurement models for ultrasonic nondestructive evaluation	Sept. 1999

List of Recent TAM Reports (cont'd)

No.	Authors	Title	Date
921	Zhang, S., and K. J. Hsia	Modeling the fracture of a sandwich structure due to cavitation in a ductile adhesive layer	Sept. 1999
922	Nimmagadda, P. B. R., and P. Sofronis	Leading order asymptotics at sharp fiber corners in creeping-matrix composite materials	Oct. 1999
923	Yoo, S., and D. N. Riahi	Effects of a moving wavy boundary on channel flow instabilities	Nov. 1999
924	Adrian, R. J., C. D. Meinhart, and C. D. Tomkins	Vortex organization in the outer region of the turbulent boundary layer	Nov. 1999
925	Riahi, D. N., and A. T. Hsui	Finite amplitude thermal convection with variable gravity—*International Journal of Mathematics and Mathematical Sciences*, in press (2000)	Dec. 1999
926	Kwok, W. Y., R. D. Moser, and J. Jiménez	A critical evaluation of the resolution properties of *B*-spline and compact finite difference methods	Feb. 2000
927	Ferry, J. P., and S. Balachandar	A fast Eulerian method for two-phase flow	Feb. 2000
928	Thoroddsen, S. T., and K. Takehara	The coalescence–cascade of a drop	Feb. 2000
929	Liu, Z.-C., R. J. Adrian, and T. J. Hanratty	Large-scale modes of turbulent channel flow: Transport and structure	Feb. 2000
930	Borodai, S. G., and R. D. Moser	The numerical decomposition of turbulent fluctuations in a compressible boundary layer	Mar. 2000
931	Balachandar, S., and F. M. Najjar	Optimal two-dimensional models for wake flows	Mar. 2000
932	Yoon, H. S., K. V. Sharp, D. F. Hill, R. J. Adrian, S. Balachandar, M. Y. Ha, and K. Kar	Integrated experimental and computational approach to simulation of flow in a stirred tank	Mar. 2000
933	Sakakibara, J., Hishida, K., and W. R. C. Phillips	On the vortical structure in a plane impinging jet	Apr. 2000
934	Phillips, W. R. C.	Eulerian space–time correlations in turbulent shear flows	Apr. 2000
935	Hsui, A. T., and D. N. Riahi	Onset of thermal–chemical convection with crystallization within a binary fluid and its geological implications	Apr. 2000
936	Cermelli, P., E. Fried, and S. Sellers	Configurational stress, yield, and flow in rate-independent plasticity—*Proceedings of the Royal Society of London A* (submitted)	Apr. 2000
937	Adrian, R. J., C. Meneveau, R. D. Moser, and J. J. Riley	Final report on 'Turbulence Measurements for Large-Eddy Simulation' workshop	Apr. 2000
938	Bagchi, P., and S. Balachandar	Linearly varying ambient flow past a sphere at finite Reynolds number—Part 1: Wake structure and forces in steady straining flow	Apr. 2000
939	Gioia, G., A. DeSimone, M. Ortiz, and A. M. Cuitiño	Folding energetics in thin-film diaphragms	Apr. 2000
940	Chaïeb, S., and G. H. McKinley	Mixing immiscible fluids: Drainage induced cusp formation	May 2000
941	Thoroddsen, S. T., and A. Q. Shen	Granular jets	May 2000
942	Riahi, D. N.	Non-axisymmetric chimney convection in a mushy layer under a high-gravity environment—In *Centrifugal Materials Processing* (L. L. Regel and W. R. Wilcox, eds.), in press (2000)	May 2000

List of Recent TAM Reports (cont'd)

No.	*Authors*	*Title*	*Date*
943	Christensen, K. T., S. M. Soloff, and R. J. Adrian	PIV Sleuth: Integrated particle image velocimetry interrogation/validation software	May 2000
944	Wang, J., N. R. Sottos, and R. L. Weaver	Laser induced thin film spallation	May 2000
945	Riahi, D. N.	Magnetohydrodynamic effects in high gravity convection during alloy solidification—In *Centrifugal Materials Processing* (L. L. Regel and W. R. Wilcox, eds.), in press (2000)	June 2000
946	Gioia, G., Y. Wang, and A. M. Cuitiño	The energetics of heterogeneous deformation in open-cell solid foams	June 2000
947	Kessler, M. R., and S. R. White	Self-activated healing of delamination damage in woven composites—*Composites A*, in press (2000)	June 2000
948	Phillips, W. R. C.	On the pseudomomentum and generalized Stokes drift in a spectrum of rotational waves	July 2000
949	Hsui, A. T., and D. N. Riahi	Does the Earth's nonuniform gravitational field affect its mantle convection?	July 2000
950	Phillips, J. W.	Abstract Book, 20th International Congress of Theoretical and Applied Mechanics (27 August – 2 September, 2000, Chicago)	July 2000
951	Vainchtein, D. L., and H. Aref	Morphological transition in compressible foam	July 2000
952	Chaïeb, S., E. Sato-Matsuo, and T. Tanaka	Shrinking-induced instabilities in gels	July 2000
953	Riahi, D. N., and A. T. Hsui	A theoretical investigation of high Rayleigh number convection in a nonuniform gravitational field	Aug. 2000
954	Riahi, D. N.	Effects of centrifugal and Coriolis forces on a hydromagnetic chimney convection in a mushy layer	Aug. 2000
955	Fried, E.	An elementary molecular-statistical basis for the Mooney and Rivlin–Saunders theories of rubber-elasticity—*Journal of the Mechanics and Physics of Solids*, to appear	Sept. 2000
956	Phillips, W. R. C.	On an instability to Langmuir circulations and the role of Prandtl and Richardson numbers	Sept. 2000
957	Chaïeb, S., and J. Sutin	Growth of myelin figures made of water soluble surfactant—Proceedings of the 1st Annual International IEEE–EMBS Conference on Microtechnologies in Medicine and Biology (October 2000, Lyon, France), 345–348	Oct. 2000
958	Christensen, K. T., and R. J. Adrian	Statistical evidence of hairpin vortex packets in wall turbulence—*Journal of Fluid Mechanics*, to appear	Oct. 2000
959	Kuznetsov, I. R., D. S. Stewart, and E. Fried	Modeling the thermal expansion boundary layer during the combustion of energetic materials—*Combustion and Flame* (submitted)	Oct. 2000
960	Zhang, S., K. J. Hsia, and A. J. Pearlstein	Potential flow model of cavitation-induced interfacial fracture in a confined ductile layer—*Journal of the Mechanics and Physics of Solids* (submitted)	Nov. 2000
961	Sharp, K. V., R. J. Adrian, J. G. Santiago, and J. I. Molho	Liquid flows in microchannels—Chapter 6 of *CRC Handbook of MEMS* (M. Gad-el-Hak, ed.) (2001)	Nov. 2000
962	Harris, John G.	Rayleigh wave propagation in curved waveguides—Elsevier preprint (submitted)	Jan. 2001
963	Dong, F., A. T. Hsui, and D. N. Riahi	A stability analysis and some numerical computations for thermal convection with a variable buoyancy factor—*Geophysical and Astrophysical Fluid Dynamics* (submitted)	Jan. 2001
964	Phillips, W. R. C.	Langmuir circulations beneath growing or decaying surface waves—*Journal of Fluid Mechanics* (submitted)	Jan. 2001